Chemical Engineering Journal 156 (2010) 366–379

Contents lists available at ScienceDirect

Chemical Engineering Journal

journal homepage: www.elsevier.com/locate/cej

Characterization and optimization of an autothermal diesel and jet fuel reformer for 5 kW_e mobile fuel cell applications

Xanthias Karatzas[a,*], Marita Nilsson[a], Jazaer Dawody[b], Bård Lindström[c], Lars J. Pettersson[a]

[a] KTH – Royal Institute of Technology, Department of Chemical Engineering and Technology, Teknikringen 42, SE-100 44 Stockholm, Sweden
[b] Volvo Technology Corporation, Chalmers Science Park, SE-412 88 Göteborg, Sweden
[c] PowerCell, Chalmers Science Park, SE-412 88 Göteborg, Sweden

ARTICLE INFO

Article history:
Received 2 June 2009
Received in revised form 15 October 2009
Accepted 18 October 2009

Keywords:
Autothermal reformer
Diesel
Fuel flow
Fuel preheating
Jet fuel
Monolithic catalyst

ABSTRACT

The present paper describes the characterization of an autothermal reformer designed to generate hydrogen by autothermal reforming (ATR) from commercial diesel fuel (~10 ppm S) and jet fuel (~200 ppm S) for a 5 kW_e polymer electrolyte fuel cell (PEFC). Commercial noble metal-based catalysts supported on 900 cpsi cordierite monoliths substrates were used for ATR with reproducible results. Parameters investigated in this study were the variation of the fuel inlet temperature, fuel flow and the H_2O/C and O_2/C ratios. Temperature profiles were studied both in the axial and radial directions of the reformer. Product gas composition was analyzed using gas chromatography.

It was concluded from the experiments that an elevated fuel inlet temperature (≥60 °C) and a higher degree of fuel dispersion, generated via a single-fluid pressurized-swirl nozzle at high fuel flow, significantly improved the performance of the reformer. Complete fuel conversion, a reforming efficiency of 81% and an H_2 selectivity of 96% were established for ATR of diesel at $P = 5\ kW_e$, $H_2O/C = 2.5$, $O_2/C = 0.49$ and a fuel inlet temperature of 60 °C. No hot-spot formation and negligible coke formation were observed in the reactor at these operating conditions. The reforming of jet fuel resulted in a reforming efficiency of only 42%. A plausible cause is the coke deposition, originating from the aromatics present in the fuel, and the adsorption of S-compounds on the active sites of the reforming catalyst.

Our results indicate possibilities for the developed catalytic reformer to be used in mobile fuel cell applications for energy-efficient hydrogen production from diesel fuel.

1. Introduction

Diesel and jet fuel are potential candidates as hydrogen carriers for fuel cells in auxiliary power units (APUs) onboard heavy-duty vehicles and aircrafts, respectively. The high energy density and existing infrastructure of the fuels make them a viable energy source for APUs. Catalytic onboard reforming technologies are considered feasible alternatives for supplying APUs with hydrogen. Autothermal reforming (ATR) has received much attention lately as one of the most promising methods for generating hydrogen from heavy hydrocarbon fuels. ATR, a thermoneutral process (see Eq. (1)), which uses air and water vapor as reactants, has several benefits in onboard reforming for mobile fuel cell applications. This is due to its high thermal efficiency (~60–75%) and dynamics during transient operation as well as the low system complexity it offers; e.g. after start-up no external heating or cooling is needed on the ATR reactor to sustain the thermoneutral process during operation [1,2].

A general reaction formula for ATR, assuming that the products (reformate) are only CO_2 and H_2, can be expressed as follows:

Autothermal reforming (ATR)

$$C_nH_m + x(O_2 + 3.76N_2) + (2n - 2x)H_2O \rightarrow nCO_2 + \left(2n - 2x + \frac{m}{2}\right)H_2 + x3.76N_2 \quad \Delta H^0 \sim 0\ kJ/mol \qquad (1)$$

For ATR, the reforming reactor design and the reforming catalyst employed are two significant factors that can determine the product gas distribution [3]. This paper discusses the development of a reactor design for ATR using diesel fuel or jet fuel. Optimal reactor design is essential to ensure complete fuel conversion, maximum hydrogen selectivity, and low amounts of carbon monoxide. Unconverted hydrocarbons and high amounts of CO are generally not desirable in APU systems as the molecules can contaminate gas purification devices and also lead to performance losses on the fuel cells, particularly for low-temperature polymer electrolyte fuel cells (PEFCs) [4]. The US Department of Energy technical targets for an onboard APU system require a durability of minimum 5000 h

* Corresponding author. Tel.: +46 8 7909150; fax: +46 8 108579.
E-mail address: xanthias@ket.kth.se (X. Karatzas).

1385-8947/$ – see front matter © 2009 Elsevier B.V. All rights reserved.
doi:10.1016/j.cej.2009.10.039

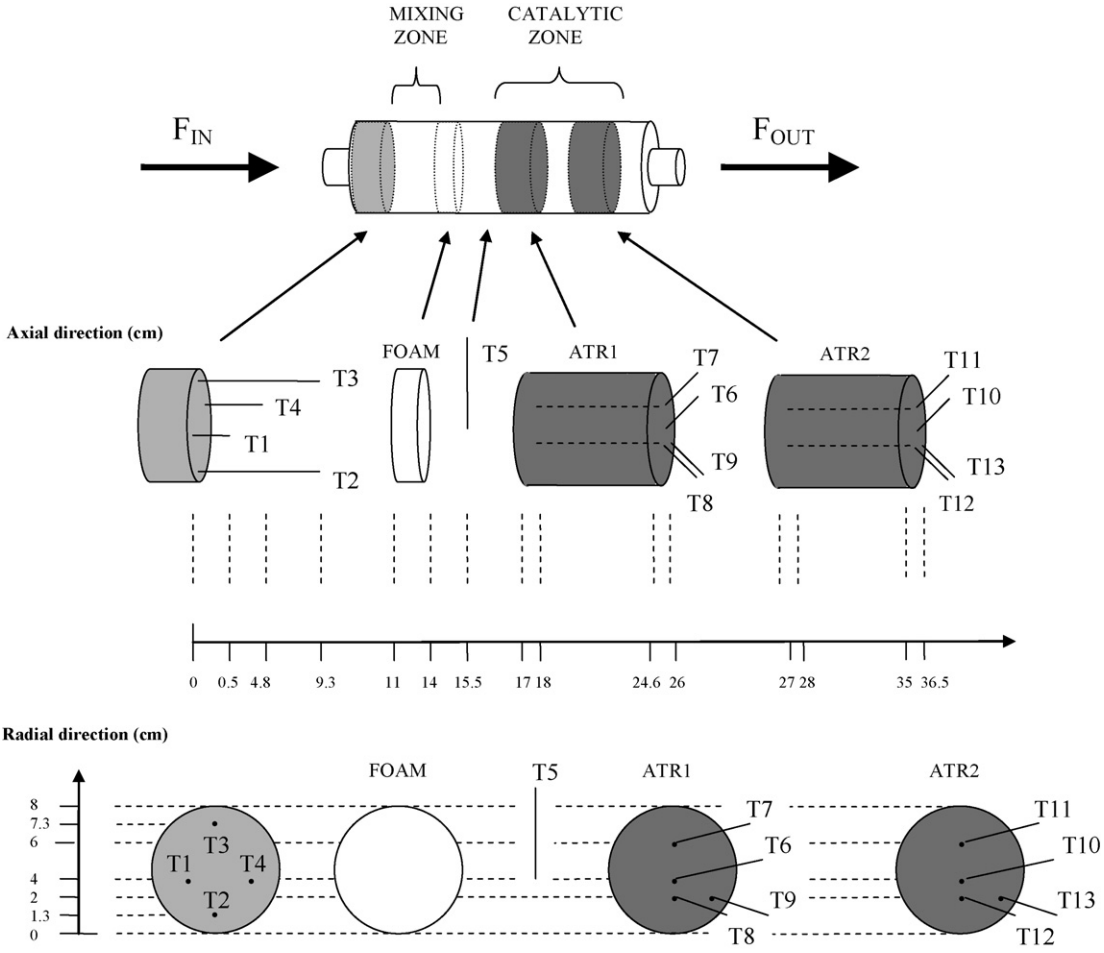

Fig. 1. Schematic drawing of the 2nd generation reformer reactor design and thermocouple set-up (T# thermocouple). FOAM = zirconia-treated alumina foam, ATR1 = first monolith in line, ATR2 = second monolith in line. Thermocouples T7, T8, T11 and T12 are placed inside the monoliths.

[4]. Thus, an optimized reformer with the right reactor design can be considered important in order to sustain the durability of the APU system.

Lately, several papers have been published where challenges concerning reactor design have been addressed. A recent paper by Porš et al. [5] show testing of different mixing chamber designs for ATR of diesel with the aim to optimize the reactant mixing and to reduce coking. In addition, a new study conducted by Kolb et al. [6] demonstrate a novel reactor concept for ATR of isooctane where stacked Rh-coated metallic platelets can offer lower pressure drop, improved heat and mass transfer and compactness of the reforming system.

Previous work performed in our laboratory has demonstrated the feasibility of reforming commercial transportation fuels (diesel, gasoline and E85) into hydrogen-rich gases. The reformer tested, herein referred to as REF1 (1st generation reformer), was capable of providing high fuel conversion (96%), reforming efficiency (61%) and H_2 selectivity (70%) during ATR of diesel [7]. Despite successful operation, improved reactor design was needed concerning fuel evaporation, reactant mixing and reforming temperature stability. In this study, a new reformer, herein referred to as REF2 (2nd generation reformer), was developed and characterized during ATR of commercial diesel fuel or jet fuel.

2. Reformer development

REF1 was designed to fulfill requirements placed on mobile fuel cell applications regarding weight, volume, simplicity, efficiency, robustness and cost. Mixture preparation is a crucial step in reforming and combustion processes. The compactness of the reforming system is also important in order to simplify heat management and to obtain high thermal efficiency. The scheme of the reactor design can be divided into two main zones: a mixing zone and a catalytic zone [8]. A single-fluid pressurized-swirl nozzle is used to inject liquid fuel as a fine spray into the mixing zone for evaporation and blending with a mixture of superheated air and steam that enters the reformer from perpendicularly arranged injection holes. The mixture then enters the catalytic zone where the reforming catalyst is located and hydrogen generation takes place. REF1 has been evaluated both experimentally and using computational fluid dynamics (CFDs) [8]. The studies showed the existence of stagnant zones of recirculated reactants in the mixing zone that lead to local hot-spot formation. These results indicated that improved turbulence, fuel dispersion and reactant mixing were needed to enhance and stabilize the reformer's performance. Based on these results a new catalytic reformer, REF2, was developed where adjustments have been made on the reactor design with the aim to improve the operating efficiency. Fig. 1 shows a schematic drawing of the new reactor design, including the thermocouple set-up. Fig. 2 shows a side view image of the new catalytic reformer used in this study.

In order to improve the fuel delivery and reactant mixing, a new single-fluid pressurized-swirl nozzle as well as a new fuel-heating device was installed. The new nozzle was expected to further atomize and disperse the fuel into the fine micro-sized droplets (<10 μm), which is predicted to increase the evaporation, mixing and combustion rates in the mixing zone. Recent papers from Porš

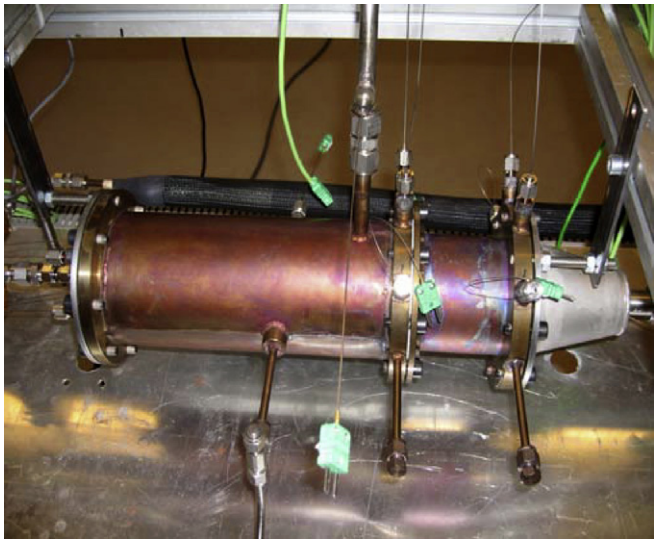

Fig. 2. Side view image of the 2nd generation reformer. The heated fuels enter from the left, and the air/steam mixture from the top of the reformer.

et al. [5] and Kang et al. [9] show the importance of choosing the right nozzle for diesel reforming in mobile fuel cell applications. Porš et al. [5] state that pressurized-swirl nozzles are preferable for diesel reforming as they exhibit less coking tendency than air-assisted nozzles. Kang et al. [9] show that the use of an ultrasonic nozzle can minimize coke formation and improve the reforming efficiency for diesel reforming. The problem with nozzles is a difficulty often faced when operating at low volumetric flows. This paper shows how the performance of the reformer is affected by the variation of the fuel flow for ATR of diesel (operated at two fixed fuel flows).

A fuel-heating device was installed to allow preheating the fuels prior to injection into the reformer. A benefit of fuel preheating is that it accelerates evaporation of the fuel spray by minimizing the droplet size. In addition, preheating lowers the viscosity and surface tension of the liquid fuel making its transportation and injection through the nozzle easier [10]. This paper demonstrates how the performance of the reformer is affected by the variation of the fuel inlet temperature.

The air–steam injection holes were repositioned further upstream in the mizing zone to prevent local hot-spot formation, i.e. to stabilize the system. Also, an alumina foam with high porosity and temperature tolerance was placed prior to the catalyst (Fig. 1) in order to further improve the reactant mixing and to prevent high concentrations of hydrocarbon fuel to come into contact with the catalyst.

The catalyst segment in the new reformer was extended by including two reforming catalysts (Fig. 1), instead of a single one in the previous reformer, with the aim of preventing fuel slip. Commercial noble metal-based catalysts supported on monolithic cordierite were chosen for testing. Noble metals are known to be very active and selective for autothermal reforming of heavier hydrocarbons [4].

This paper focuses on the characterization and optimization of REF2. The variation of the fuel flow and the effects of fuel preheating were studied in particular. Test fuels were commercial diesel and jet fuel.

3. Experimental

3.1. The 2nd generation reformer

The 2nd generation reformer consists of a stainless steel tubular reactor with 84 mm inner diameter and 400 mm length (Figs. 1 and 2) horizontally mounted. The walls of the reactor were insulated with alumina–silica blanket insulation to minimize

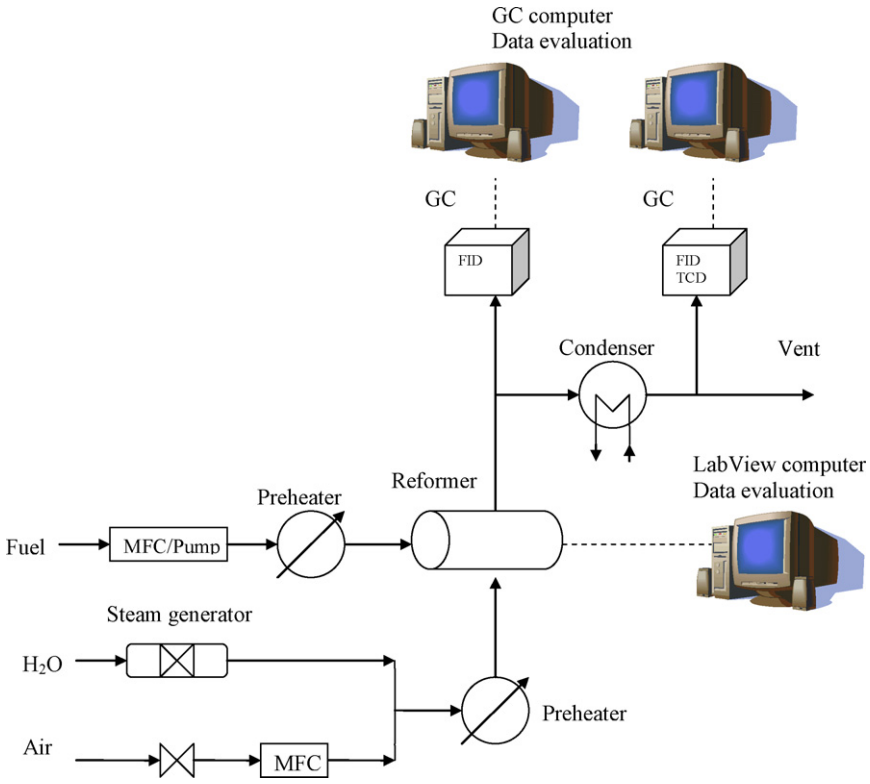

Fig. 3. Experimental set-up for autothermal reforming of preheated liquid fuels.

heat losses. Fig. 3 shows the experimental set-up for autothermal reforming of preheated liquid fuels. The liquid fuel was delivered to the reformer using an electronically controlled piston pump (0–65 cm^3/min, 6.9 bar maximum pressure, Fluid Metering Inc.). A heating hose made of corrugated steel with 62 mm outer diameter and 1500 mm length (0–600 °C, 450 W maximum power, H 900 series, Hillesheim) and a temperature controller (HT43, Hillesheim) were used to regulate the fuel inlet temperature.

The preheated liquid fuel was injected through a stainless steel spray nozzle (0.23 mm diameter, MistJet®, STEINEN) generating a hollow-cone spray of fuel with a spread angle of approximately 70°. Following injection, the fuel was vaporized in a mixture of air and steam that had been superheated to a temperature of 300 °C enabling fuel vaporization. The air-steam mixture is delivered through a mantle around the reactor, enabling indirect heat exchange with the reformer; it enters the mixing zone through injection holes positioned near the nozzle. The superheating was performed in a separate unit by means of tubular heating elements. Gases were fed to the reformer using mass flow controllers (Bronkhorst High-Tech EL-Flow model).

A zirconia-treated alumina foam with 80.3 mm diameter and 26.4 mm length (RQ-3085, Selee Corp.) is placed prior the catalyst to enhance the reactant mixing and to protect the catalysts. The catalysts, herein referred to as ATR1 and ATR2, were commercial noble metal supported on a 900 cpsi cordierite monolith with 80.3 mm diameter and 76.2 mm length. A heat-resistant packaging mat (KZ Handels AB) covered the inside of the reactor to hold the foam and the monoliths in place, also minimizing leakages around the catalysts. Three high temperature-tolerant plug valves (6 mm, Swagelok) are attached perpendicularly on the reformer (not shown in Fig. 2). The valves are placed after the foam, ATR1 and ATR2, respectively, to collect gas samples for analysis.

3.2. ATR of diesel and jet fuel experiments

Experiments were performed in a reactor designed to generate hydrogen by autothermal reforming from commercial diesel (~10 ppm S) and jet fuel (~200 ppm S) for a 5 kW_e PEFC. Table 1 shows the properties of the liquid fuels used in this study. Parameters investigated in this study were the variation of the fuel inlet temperature (FIT), fuel flow, H_2O/C and O_2/C ratios.

The experiments were essentially divided into three parts. The first two parts concern autothermal reforming of diesel where two different fuel flows, 13 and 18.5 g/min (electrical power output for PEFC, P = 3 and 5 kW_e), and the effect of fuel preheating was tested and studied. The final part concerns autothermal reforming of jet fuel at a constant fuel flow, 18.5 g/min (P = 5 kW_e), also including fuel preheating testing. The operating conditions used in this study are described in detail in Table 2.

3.3. Operational considerations

The first step in the evaluation of the reformer was to explore and determine the operating parameters of the autothermal reforming process to obtain optimal efficiency. For ATR, the steam-to-carbon (H_2O/C) and oxygen-to carbon ratios (O_2/C) are two of the most significant operating parameters that are often initially determined. A high H_2O/C ratio is desirable as steam cleanses the reactor's inner walls, the foam surface and the catalyst active sites from carbonaceous species. Generating a high H_2O/C ratio can be costly, as more time, energy and larger volumes of water are required to generate sufficient steam. The O_2/C ratio is also important as oxygen improves the dynamic response of the reformer. The O_2/C ratio regulates the reforming temperature in the reactor. Too high O_2/C may lead to total oxidation of the fuels (Eq. (2)), resulting in hydrogen loss.

Table 1
Comparison of properties for the fuels tested in the study [11–15].

	Diesel	Jet A-1
Chemical formula	~$C_{14}H_{26}$	~$C_{11}H_{21}$
Molecular weight (g mol^{-1})	~194	~153
Boiling point at 1 bar (°C)	180–290[a]	166–266
Vapor pressure at 38 °C (bar)	Negl.	Negl.
Liq. density at 15 °C (kg m^{-3})	800–820	775–840
Liq. viscosity at 25 °C (mPa s)	2–4	~3.5($^{(-20\,°C)}$)
Heat of vaporization (MJ/kg)	0.27	0.30
Lower heating value (MJ/kg)	43	43
Autoignition temperature (°C)	206[b]	210–220
Flammability limits in air (vol%)	1–5	1–6
Sulfur content max (wt% ppm)	0–10	~200
Aromatic content max (vol%)	5	19.5

[a] T95.
[b] n-Cetane.

Total oxidation

$$C_xH_y + \left(x + \frac{1}{4}y\right)(O_2 + 3.76N_2) \rightarrow xCO_2 + \frac{1}{2}yH_2O + \left(x + \frac{1}{4}y\right)3.76N_2 \quad \Delta H^0 < 0\,\text{kJ/mol} \tag{2}$$

Thermodynamic equilibrium calculations, e.g. by using NASA CEA software, show that maximum hydrogen productivity for ATR of diesel and jet fuel is obtained in the temperature region of 700–750 °C [8]. Although ATR is a thermally neutral process the O_2/C ratio is often kept slightly higher than the thermodynamic equilibrium value in order to promote the oxidation reactions that initiate the process and to compensate for heat losses. Several studies have shown that the exothermic partial oxidation reaction initiates autothermal reforming, see Eq. (3) [9,13]. This is due to the faster kinetics of the partial oxidation reaction. Heat generated from partial oxidation is consumed by subsequent endothermic steam reforming, where most of the hydrogen is generated; see Eq. (4). For this study H_2O/C and O_2/C ratios were initially determined for all commercial fuels tested.

Partial oxidation (PO)

$$C_xH_y + \frac{1}{2}x(O_2 + 3.76N_2) \rightarrow xCO + \frac{1}{2}yH_2 + \frac{1}{2}x3.76N_2 \quad \Delta H^0 < 0\,\text{kJ/mol} \tag{3}$$

Table 2
Operating parameters for the fuels used in this study.

Fuel	FIT[a] (°C)	Flow rate (g fuel min^{-1})	P[b] (kW_e)	O_2:C (mol/mol)	λ[c]	H_2O:C (mol/mol)	GHSV (h^{-1})
Diesel[d]	25–60–100–120–130	13.0	3	0.49	0.33	2.5	7,600
Diesel[d]	25–60–100–120	18.5	5	0.49	0.33	2.5	10,800
Jet fuel[e]	25–60	18.5	5	0.39	0.25	2.1	9,000

[a] FIT = fuel inlet temperature.
[b] P = electric power output for a PEFC.
[c] λ = actual-to-stoichiometric air/fuel ratio.
[d] Swedish Environmental Class 1 (MK1).
[e] Aviation fuel, jet A-1.

Steam reforming (SR)

$$C_xH_y + xH_2O \rightarrow xCO + \left(x + \frac{1}{2}y\right) H_2 \quad \Delta H^0 > 0 \text{ kJ/mol} \tag{4}$$

The second phase of this study concerns evaluating the effect of preheating the fuels on the performance of the reformer. The fuel inlet temperature was varied at fixed stages to examine the overall effect. Temperature monitoring and gas analysis of the reformate was carried out after each stage, at steady-state conditions. Fuel preheating is expected to have a beneficial impact on the combustion and mixing reactions occurring in the mixing zone. Heat and mass transfer correlations can be employed to explain the fundamentals for these types of reactions. The Chilton–Colburn analogy can be used to predict the driving force for the evaporation rate of liquid fuel. Assuming the injected droplets are in the shape of spheres, the simplified Eq. (5) can be implemented to calculate the evaporation rate (W_{A0}) for a liquid (A)–gas (B) system. The equation assumes quasi-steady state and constant surface temperature and composition [10]:

$$W_{A0} = k_{xm}(\pi D^2)\frac{x_{A0}x_{A\infty}}{1 - x_{A0}} \tag{5}$$

where x_{A0} and $x_{A\infty}$ are the initial and final vapor pressure conditions in liquid surface film. The mean mass transfer coefficient (k_{xm}), which is the most influential factor in the evaporation rate, is defined as follows [10]:

$$k_{xm} = \frac{cD_{AB}}{D}Sh_m \quad (Sh_m = Sheerwood\,number) \tag{6}$$

Heating on and increased velocity of the liquid droplet lead to greater tension and friction on the periphery, which decreases the droplet diameter (D) and consequently increases k_{xm}. The mean mass transfer coefficient is also affected by an increase of pressure and temperature of the gas system. As a result, the concentration of the gas (c) and the diffusion coefficient of the liquid in gas (D_{AB}) both increase, which accelerates the vaporization. In this study, the reactor inlet pressure and the air–steam mixture temperature were held at 1 bar and 300 °C, respectively, for all experiments. Studies have shown that the variation of the pressure does not affect the product gas composition for ATR of diesel [5]. Diesel is a liquid mixture of different hydrocarbon groups, such as paraffins, olefins and aromatics (see Table 1). The various compounds in the fuel make it difficult to use heat and mass transfer correlations. In addition, diesel, due to its many ingredients, has a wide boiling range with an initial boiling point of ~180 °C. In this study, the maximum fuel inlet temperature for diesel was set to 130 °C (see Table 2).

The third phase of this study concerns evaluating the effect of fuel-flow variation on the performance of the reformer. Two fixed fuel flows of diesel, 13 and 18.5 g/min (P = 3 and 5 kW_e) were tested and studied. A higher volumetric flow may generate smaller droplets in the spray and consequently lead to faster fuel evaporation (Eqs. (5)–(6)). Also, a higher volumetric flow may improve the fuel dispersion in the radial direction, which can enhance the mixing of diesel with the air/steam mixture. On the other hand, an increased fuel flow could also lead to excessively strong jet of fuel which would wet and block the surface of the foam. The reformer injection system was therefore calibrated prior to each experiment to generate spray at desired operational conditions.

Finally, ATR of jet fuel was carried out at a fuel flow of 18.5 g/min, corresponding to constant power output of 5 kW_e for a PEFC (Table 2). Jet fuel, jet A-1, was chosen as test fuel since its overall physical properties are similar to those of diesel, see Table 1. The similarities in viscosity, boiling point, lower heating value and density meant the fuel delivery and mixture preparation of jet A-1 would be comparable to the experimental procedure employed for diesel. Differences in results would mainly be attributable to the chemical composition of the jet A-1, such as contents of sulfur and aromatics.

The higher sulfur concentration in jet A-1, and its influence on the autothermal reforming process was of interest to study. Typical sulfur compounds in jet A-1 are benzothiophene, C1–C3 benzothiophene and C2–C3 thiophene [16,17]. Sulfur is known to have a poisoning effect on the catalyst performance due to adsorption of S-compounds, such as H_2S and SO_2, on the active sites of the catalyst. Hydrogen sulfide is converted from hydrocarbons in a non-oxidizing environment while sulfur dioxide products are generated in an oxidizing environment [4]. Thus, in autothermal reforming there is possibility of co-existence of both sulfur compounds in the reformate. Cimino et al. [18] investigated the catalyst poisoning effect using H_2S and SO_2 as sulfur compounds for PO of CH_4 over noble metal-based catalyst and found that the catalyst were merely affected by the total S concentration in the feed and not by the type of sulfur precursor. Similar results were observed by Cheekatamarla and Lane [19] where synthetic diesel, together with H_2S and SO_2, was tested for ATR using noble metal-based catalyst. Studies have also shown that sulfur can have a detrimental effect, not only on the catalyst employed, but also on the reformer fuel injection system [20]. Sulfur can also affect the performance of the fuel cell. Hydrogen sulfide is reported to have a more severe poisoning on PEFC compared to carbon monoxide; 1 ppm can decrease the efficiency of the fuel cell by preferential adsorption on the electrodes [21]. Often a desulfurization step is carried out prior to the reforming process. Also, a reaction temperature above 800 °C can be implemented to prevent sulfur adsorption on the reforming catalyst but at the cost of hydrogen loss [22].

The higher aromatic content in jet fuel, compared to diesel, impacts the reforming process; it was also expected to affect the catalyst performance. Typical aromatic compounds in jet A-1 are benzene, C1–C3 benzene, toluene and xylenes [23]. These products have also been reported to be present in jet fuel reformates [20] as well as in emissions from aircrafts [24]. In reforming, aromatics are known to be less reactive, due to stable C–C and C–H bonds, and to have higher coking tendency than paraffins [25]. Flytzani-Stephanopoulos and Voecks [26] investigated the effect of coke poisoning for ATR of benzene over Ni monolithic catalyst. Their result showed that coke was present on the catalyst, low conversion of benzene was achieved, and low amounts of olefins were found in the bed. The main product was methane. They came to the conclusion that the main coke precursor was not the olefins, but the aromatic molecule itself. They suggest that benzene forms carbon through dehydrogenation in the gas phase in the monolith channels at high temperatures.

A synergistic effect between sulfur and aromatics has also been studied for instance by McCoy et al. [27]. A fuel blend consisting of toluene and 50 ppm thiophene was tested for ATR over Rh- and Pd-based catalyst. Their results showed a steady decrease of the H_2 yield for all catalysts over a duration of 24 h. In addition, Rh showed higher activity and better resistance towards sulfur.

Thus, taking the aromatic and sulfur poisoning effect into account, it is vital to establish the right reaction conditions for ATR of jet A-1, e.g. to establish a high H_2O/C to suppress coke formation and a high reaction temperature to prevent sulfur adsorption. In this study, the operating parameters for autothermal reforming of jet A-1 were collected from literature data [28–30]. It can be emphasized that limited information can be found in the open literature where non-desulfurized treated commercial jet fuel has been tested for autothermal reforming.

All experiments were run until stable and reproducible results were obtained. Typical time on stream ranged from 2 to 7 h. Steady-state conditions were reached approximately 30 min after start-up of the reformer. During shutdown of the reformer, the air was shut off first, followed by fuel and steam. Air was then flushed through

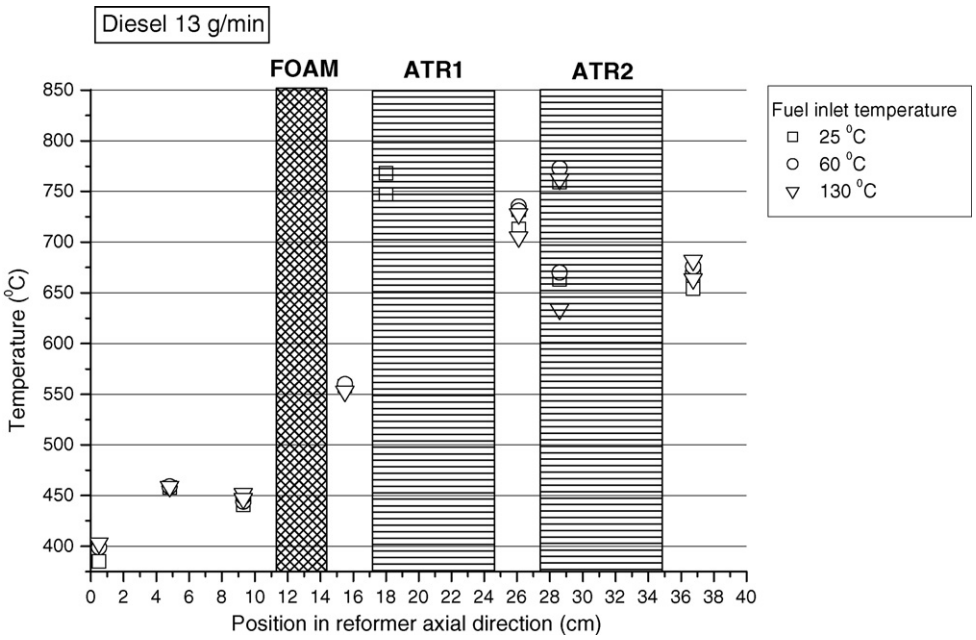

Fig. 4. Temperatures in the reactor during autothermal reforming of commercial diesel at different fuel inlet temperatures. Fuel flow = 13 g/min, $H_2O/C = 2.5$, $O_2/C = 0.49$, GHSV = 7600 h^{-1} (positions of the thermocouples are shown in Fig. 1). FOAM = zirconia-treated alumina foam, ATR1 = first monolith in line, ATR2 = second monolith in line.

the reformer to burn off potential coke and sulfur on the catalyst surface. Coke and sulfur compounds, e.g. H_2S and SO_2, could then be detected by increases in temperature after the monolith, see Eqs. (7)–(9). An ocular inspection of the nozzle interior, alumina foam, reforming catalyst and the inside of the reactor walls was also performed after each experiment.

Oxidation of coke

$$C + O_2 \rightarrow CO_2 \quad \Delta H^0 < 0\,\text{kJ/mol} \tag{7}$$

Oxidation of H_2S

$$H_2S + 3/2O_2 \rightarrow H_2O + SO_2 \quad \Delta H^0 < -518.2\,\text{kJ/mol} \tag{8}$$

Oxidation of SO_2

$$SO_2 + 1/2O_2 \rightarrow SO_3 \quad \Delta H^0 < -99\,\text{kJ/mol} \tag{9}$$

3.4. Collection of data

Temperature profiles were studied using K-type thermocouples placed in the mixing zone (T1–T4 in Fig. 1), after the alumina foam (T5 in Fig. 1), inside the monolithic channel (T7–T8 for ATR1 and T11–T12 for ATR2 in Fig. 1) and after the catalysts (for ATR1 T6, T9 and for ATR2 T10, T13 in Fig. 1). The thermocouples T7, T8, T11 and T12 (ID = 0.5 mm) were placed inside the monolith channels' front part to measure the temperature of the reformate and to register temperature rises caused by the exothermic PO. In addition a thermocouple (not shown in Fig. 1) was placed prior to the reformer to measure the fuel inlet temperature.

The reactor effluent product compositions were studied by gas chromatography (GC), using a Varian CP-3800 and a Varian 3400CX. The CP-3800 is equipped with a thermal conductivity detector (TCD) and a flame ionization detector (FID) and two packed columns, a Porapak Q and a MS 5A where CH_4, CO, CO_2, H_2, N_2, and O_2 can be quantitatively analyzed. The 3400CX is equipped with two capillary columns, a VF-1ms and a GS-Q and two FIDs. This GC was used for detection of the higher molecular weight hydrocarbons present in the wet reformate (see Fig. 3).

3.5. Analysis of results

The following equations were used for evaluation of the data, with F corresponding to molar flows (mol/min):

$$H_2 \text{ selectivity } (\%) = \frac{F_{H_2+CO}}{F_{H_2,\max}} \times 100 \tag{10}$$

$$\text{Fuel conversion } (\%) = \frac{F_{C_xH_y,\text{in}} - F_{C_xH_y,\text{out}}}{F_{C_xH_y,\text{in}}} \times 100 \tag{11}$$

$$O_2 \text{ conversion } (\%) = \frac{F_{O_2,\text{in}} - F_{O_2,\text{out}}}{F_{O_2,\text{in}}} \times 100 \tag{12}$$

$$CO_2 \text{ selectivity parameter } (\%) = \frac{F_{CO_2}}{F_{CO_2} + F_{CO}} \times 100 \tag{13}$$

The hydrogen selectivity (Eq. (10)) was defined as the molar flows of hydrogen plus carbon monoxide in the product gas obtained per mole of fuel divided by the theoretical maximum hydrogen flow, per mole of the fuel, at the specific condition (assuming all carbon reacts to CO_2). The hydrogen selectivity equation is defined and written from an APU system point of view where CO can be converted in the fuel processor to H_2 and CO_2 [4].

The fuel conversion was estimated by means of atomic carbon balances (Eq. (11)) where diesel fuel is assumed to consist solely of $C_{14}H_{26}$ and jet A-1 of $C_{11}H_{21}$ (see Table 1). The $CO_2/(CO_2 + CO)$ product ratio (Eq. (13)) was used as a parameter to evaluate the selectivity to CO_2 relative to CO, not including other carbon-containing components such as CH_4 and unconverted hydrocarbons.

The reforming efficiency (η) was calculated according to the following equation (lower heating values of the fuels, LHV, are shown in Table 1):

$$\eta = \frac{(F_{H_2} + F_{CO})\text{LHV}_{H_2}}{F_{\text{fuel}}\text{LHV}_{\text{fuel}}} \times 100 \quad \text{LHV}_{H_2} = 242\,\text{kJ/mol} \tag{14}$$

Table 3
Fuel and oxygen conversions (mol%) after monoliths ATR1 and ATR2, diesel flows 13 g/min and 18.5 g/min. $H_2O/C = 2.5$, $O_2/C = 0.49$. FIT = fuel inlet temperature.

Diesel 13 g/min					Diesel 18.5 g/min				
	ATR1		ATR2			ATR1		ATR2	
FIT (°C)	Fuel conversion (mol%)	O_2 conversion (mol%)	Fuel conversion (mol%)	O_2 conversion (mol%)	FIT (°C)	Fuel conversion (mol%)	O_2 conversion (mol%)	Fuel conversion (mol%)	O_2 conversion (mol%)
25	56	64	99	89	25	94	87	100	92
60	86	79	100	93	60	100	93	100	95
100	100	94	100	94	100	100	95	100	95

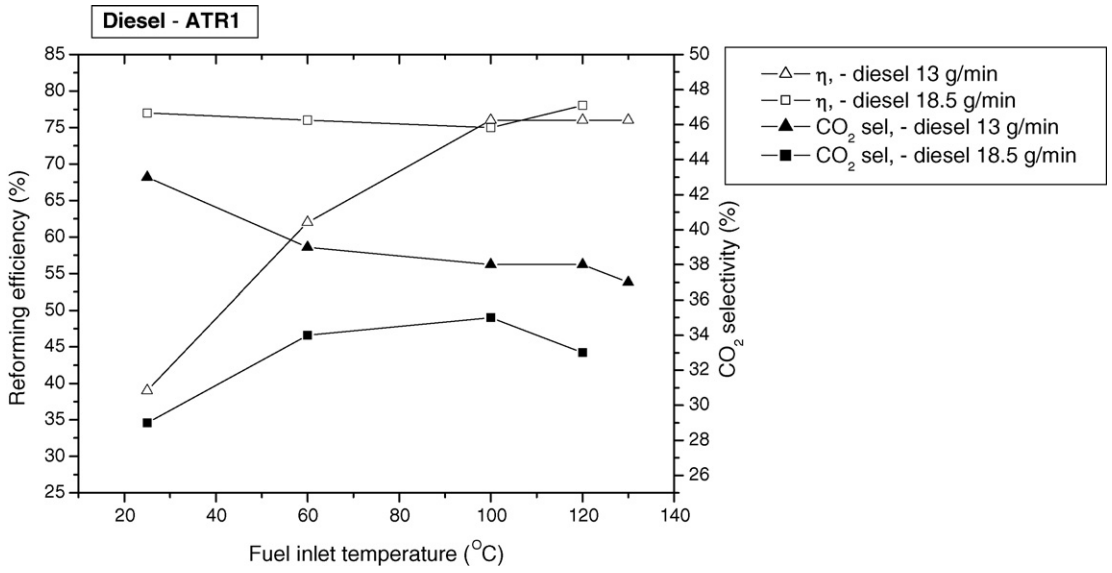

Fig. 5. Autothermal reforming of commercial diesel, ATR1 (first monolith in line in the reactor). Comparison of different fuel flows and fuel inlet temperatures on the reforming efficiency (η) and CO_2 selectivity at $H_2O/C = 2.5$, $O_2/C = 0.49$.

4. Results and discussion

4.1. Diesel reforming, fuel flow 13 g/min

Fig. 4 shows the reactor temperature profiles obtained from operation at a fuel flow of 13 g diesel/min at steady-state conditions. The temperatures registered in the mixing zone range from 400 to 460 °C. Increasing the fuel inlet temperature (FIT) from 25 to 130 °C resulted in a small temperature increase of ~15 °C for the thermocouple located nearest to the nozzle (T1 in Fig. 1). The foam placed prior to the catalyst enhances the mass and heat transfer between the reactants, which results in a temperature increase of the mixture up to ~500 °C. Furthermore, the temperature rise could also be due to heat radiation from the front part of the first mono-

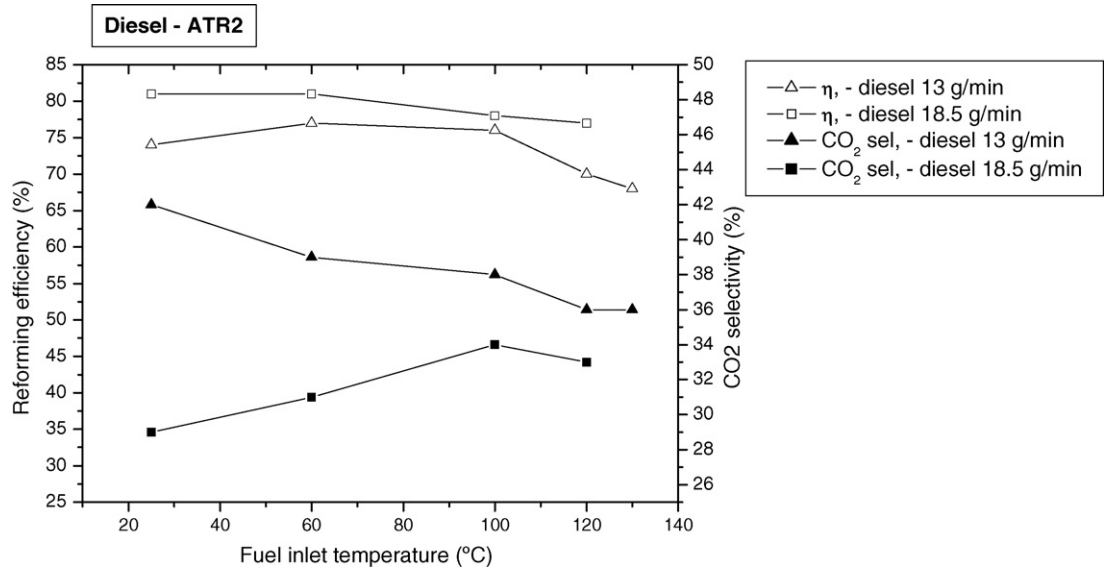

Fig. 6. Autothermal reforming of commercial diesel, ATR2 (second monolith in line in the reactor). Comparison of different fuel flows and fuel inlet temperatures on the reforming efficiency (η) and CO_2 selectivity at $H_2O/C = 2.5$, $O_2/C = 0.49$.

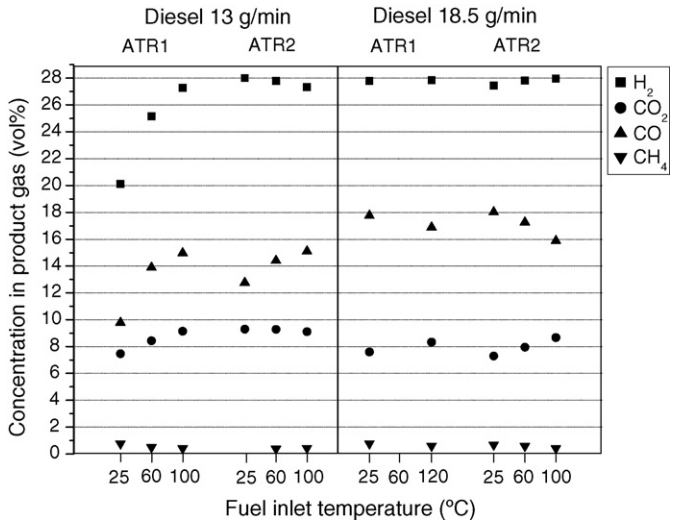

Fig. 7. Product gas concentrations of H_2, CO_2, CO, and CH_4 (dry reformate) measured after both monoliths, ATR1 and ATR2, at two diesel flows and various fuel inlet temperatures. $H_2O/C = 2.5$, $O_2/C = 0.49$.

lith emanating from exothermic reactions. For instance, Liu et al. [31] have made a similar observation.

The two thermocouples located inside the front part of the first monolith (T7, T8, ATR1) registered a significant temperature rise up to 750 °C. The temperature rise may be the result of catalytic exothermic partial oxidation (PO). All experiments using diesel at a flow of 13 g/min showed the same temperature trend. The thermocouples inside ATR1 were thermally destroyed after approximately 30 h reforming. As a result, no temperature data could be obtained for FIT 60 and 130 °C. The thermocouples were replaced before the tests using jet A-1. The temperature after ATR1 was 705–730 °C, which lies in the thermodynamically favored region for maximum hydrogen productivity [8]. For the second monolith (ATR2), the two thermocouples located inside the monolithic channels (T11–T12) registered considerably different gas phase temperatures (663–773 °C). The temperature after ATR2 was 650–680 °C. The decrease in the temperature is most likely the result of heat consumption due to endothermic steam-reforming (SR) activity. This declining temperature trend was also recently reported by Liu et al. [21] for autothermal reforming for reactors containing series of monolithic catalysts. Also, Flytzani-Stephanopoulos and Voecks [26] have reported similar temperature trend results.

Table 3 shows the fuel and oxygen conversion measured after each monolith. The difference in the fuel and oxygen conversions may be the cause of the difference in temperature inside the monolith channels, previously mentioned. A possible explanation is that unconverted oxygen and hydrocarbons after ATR1 react inside ATR2 thus giving rise to the temperature gradient. Table 3 also shows that an increase in the fuel inlet temperature improves the fuel and oxygen conversions, particularly over ATR1. It is also interesting to note that despite not having achieved full conversion of O_2, a fuel conversion of 100% is obtained after ATR1. Liu et al. [31] presented similar results where a series of four monolithic catalysts were tested for diesel reforming. Results from their study show full conversion of oxygen was not achieved after the first monolith and still very high H_2 production close to 30 vol% was reached. Also, Flytzani-Stephanopoulos and Voecks [26] reported in their ATR experiments with n-tetradecane that not all oxygen was consumed in their first catalyst in a series of Ni supported monolithic catalyst.

Figs. 5 and 6 show the reforming efficiency (η) and CO_2 selectivity and Fig. 7 displays the product gas distributions (dry reformate) measured after both monoliths.

After ATR1, a reforming efficiency of only 40% is obtained at the initial fuel inlet temperature (FIT = 25 °C, see Fig. 5) as a result of the incomplete conversion of diesel and oxygen (see Table 3). By increasing the fuel inlet temperature to 60 °C the reforming efficiency is significantly improved (62%), as a result of generating more H_2 and CO (see Fig. 7). As more CO is formed the CO_2 selectivity decreases steadily (see Fig. 5). Also, the CH_4 formation decreases (see Fig. 7). Complete fuel conversion (see Table 3) and a reforming efficiency of 75% (see Fig. 5) are achieved at a fuel inlet temperature of 100 °C. The H_2, CO, CO_2 and CH_4 production at this operational condition was as follows (Fig. 7): 27.5, 15, 9 vol% and 430 ppm (vol). The remainder of the analyzed dry gas composition is nitrogen. In addition, very small stable quantities of C2- and C4-compounds (<50 ppm) without an increase over time on stream, were detected in the wet reformate. Further fuel preheating had minor impact on performance of ATR1.

For ATR2, very high fuel conversion (~99%) (see Table 3), a reforming efficiency ~74% (see Fig. 6) and the H_2 concentration 28 vol% (see Fig. 7) are achieved already at the fuel inlet temperature 25 °C. No higher hydrocarbon molecules, such as C2- and C4-compunds, were detected in the analyzed gas composition of the wet reformate. Further fuel preheating slightly improved the oxygen conversion, as seen in Table 3.

Coke formation was detected in ATR1 during shutdown while pulsing oxygen through the reformer. The highly exothermic reactions noted during coke removal destroyed thermocouples T7–T8 as the maximum operating temperature of the materials (1200 °C) was exceeded. It is possible that coke may have been originated from the unconverted hydrocarbons and C2- and C4-compounds present in the wet reformate from ATR1, as previously discussed. Efforts were made to identify the byproducts formed during diesel reforming. Acetaldehyde, ethylene, ethane, acetic acid and propane were injected into the GC, but could not be separated adequately to enable identification of the samples from the experiments. Traces of carbonaceous material were also found in the condensate. In addition, fuel inlet temperatures above 120 °C resulted in minor coke deposition inside the filter in the nozzle. The coke was scraped from the nozzle and the weight of the sample was measured using a scale. The coke weight was 0.130 g which corresponded to 0.5 wt% increase of the total weight of the nozzle. Porš et al. [5] report that high wall temperatures inside the nozzle can lead to coke deposition. In this study, it seems that heat transfer from preheated fuels raises the inner wall temperatures of the nozzle, which accelerate carbon formation. Continuous external cooling of the nozzle system can be a possible method to circumvent this problem.

Fig. 8 shows the front part of the alumina foam after the final experiment using a diesel flow of 13 g/min. The center of the surface of the foam is slightly darkened. This indicates that the spreading angle of the diesel spray was not fully achieved. Instead, the spray may be centered, due to accumulated droplets, and not properly mixed with air/steam and consequently exposed to the center of the foam, as seen in Fig. 8. The insufficient mixture preparation is believed to cause the low fuel and oxygen conversions over ATR1, as previously discussed. Based on this observation an increase of the volumetric flow of diesel was required to improve the dispersion of the fuel. Hence, a diesel flow of 18.5 g/min was tested using the same steam-to-carbon ($H_2O/C = 2.5$) and oxygen-to-carbon ($O_2/C = 0.49$) ratios. The higher fuel flow decreases the residence time of the heated liquid diesel in the nozzle which is expected to lower the tendency for carbon formation [5].

Based on the results from ATR of diesel 13 g/min, the fuel delivery can be considered a significant factor for diesel reforming. For the first monolith (ATR1), the incomplete reactant mixing, due to poor fuel dispersion, is believed to cause low fuel conversion, reforming efficiency and hydrogen production. Results show that an increase in the fuel inlet temperature significantly improves the

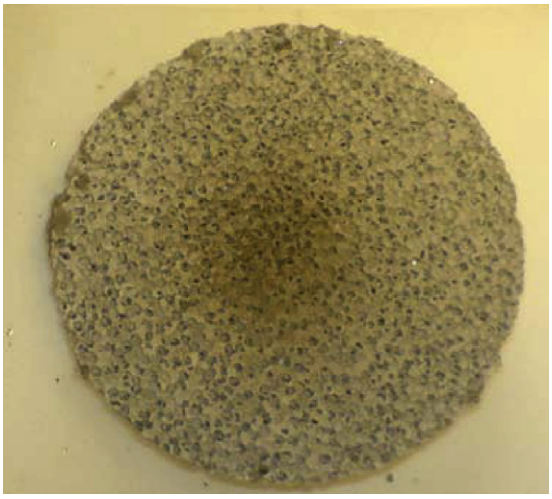

Fig. 8. Zirconia-treated alumina foam from autothermal reforming of diesel, 13 g/min at $H_2O/C = 2.5$, $O_2/C = 0.49$ after final experiment.

fuel and oxygen conversion over ATR1. Fuel preheating is believed to improve the fuel dispersion and evaporation and thus the reactant mixing is improved. For the second monolith (ATR2), maximal operating efficiency is obtained at the initial fuel inlet temperature (FIT = 25 °C). Fuel preheating had a slightly positive impact on the oxygen conversion.

4.2. Diesel reforming, fuel flow 18.5 g/min

Fig. 9 shows the temperature profile from operation of diesel at 18.5 g/min at steady-state conditions. The temperature gradient in the axial direction in the mixing zone was only 25 °C compared to 50 °C at a fuel flow of 13 g/min. This regardless of the fuel inlet temperature employed. The lower temperature gradient may be attributed to an improved dispersion and smaller droplets of the diesel at the higher flow rate which result in enhanced fuel evaporation and mixing. In addition, the higher diesel and oxygen load assists and accelerates the heat and mass transfer that takes place in the mixing zone. The temperature after the foam was constant at ~590 °C, this regardless of the fuel inlet temperature employed. Compared to the ATR of diesel at fuel flow 13 g/min, the thermocouples located inside the monolith channels in ATR2 (T11–T12) showed a significantly lower temperature gradient (753–808 °C). This is believed to be due to the improved fuel and oxygen conversions in ATR1, which can be seen in Table 3. The temperature of the gas after ATR2 was 705–715 °C. The decrease in temperature is likely the result of steam-reforming activity.

Table 3 and Figs. 5 and 7 show that most of the reforming reactions occur in the first monolith. Most of the fuel and oxygen are converted (Table 3), and also the expected end products are formed in the reformate (Fig. 7), after the first monolith at FIT = 25 °C. These fuel, oxygen and product gas composition trends are in good agreement with what has been reported by Flytzani-Stephanopoulos and Voecks [26] and Liu et al. [31]. Also, the higher GHSV for diesel at 18.5 g/min, which means lower residence time for gaseous reactants to adsorb, react and desorb in the monolith channels, does not seem to affect the product gas composition in the reformate.

For ATR1, complete fuel conversion (see Table 3), a reforming efficiency of ~76% (see Fig. 5) and an H_2 concentration of 28 vol% (see Fig. 7) are achieved at fuel inlet temperature of 60 °C. Similar results are observed after ATR2. For ATR2, the highest reforming efficiency (81%) is achieved at fuel inlet temperatures of 25 and 60 °C (see Fig. 6). Also, for both monoliths the CH_4 formation decreases with an increase of the fuel inlet temperature (see Fig. 7). No higher hydrocarbon molecules, such as C2- and C4-compounds, were detected in the analyzed gas composition of the wet reformate from both monoliths.

Interestingly, for both ATR1 and ATR2, the concentrations of H_2 and CO in the dry reformate increase and decrease slightly, respectively, as the fuel inlet temperature increases (see Fig. 7). In addition, the CO_2 selectivity increases (see Figs. 5 and 6). These trends could be an indication of water-gas shift (WGS) activity (see Eq. (15). This activity has been reported in the literature by Kaila et al. [22] and Abu-Jrai et al. [32] for autothermal reforming of diesel in the reforming temperature region of 700–800 °C:

Water-gas shift (WGS)

$$CO + H_2O \leftrightarrow CO_2 + H_2 \quad \Delta H^0 = -42\ \text{kJ/mol} \tag{15}$$

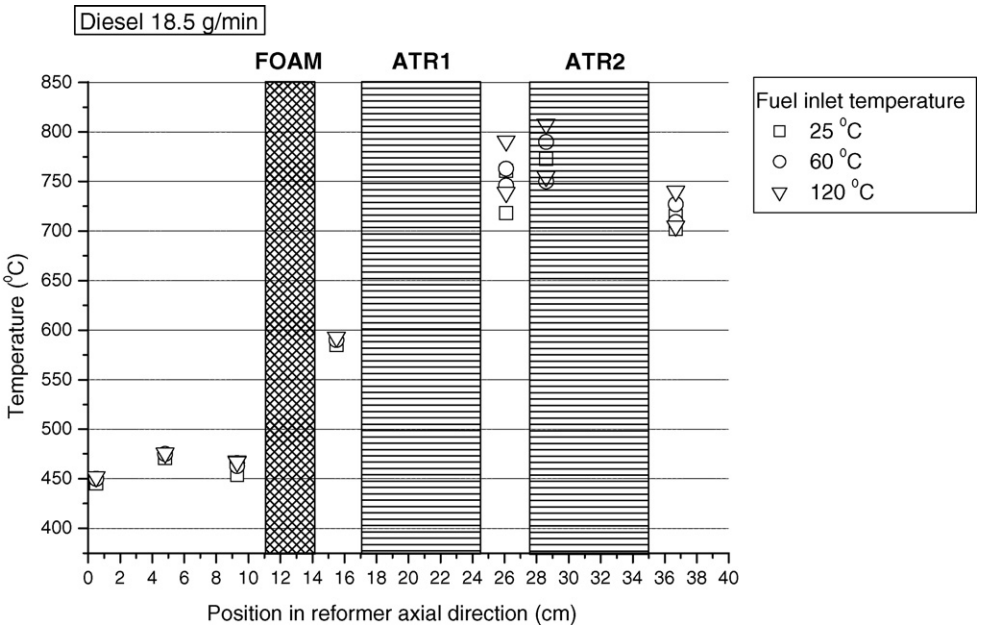

Fig. 9. Temperatures in the reactor during autothermal reforming of commercial diesel at different fuel inlet temperatures. Fuel flow = 18.5 g/min, $H_2O/C = 2.5$, $O_2/C = 0.49$, GHSV = 10,800 h^{-1} (positions of the thermocouples are shown in Fig. 1). FOAM = zirconia-treated alumina foam, ATR1 = first monolith in line, ATR2 = second monolith in line.

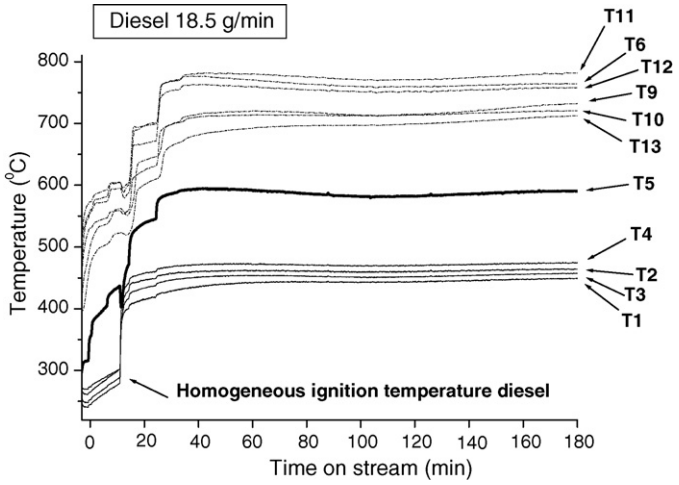

Fig. 10. Temperatures in the reactor vs. time on stream at fuel inlet temperature 25 °C. Diesel flow 18.5 g/min. $H_2O/C = 2.5$, $O_2/C = 0.49$, GHSV = 7600 h^{-1} (positions of the thermocouples are shown in Fig. 1).

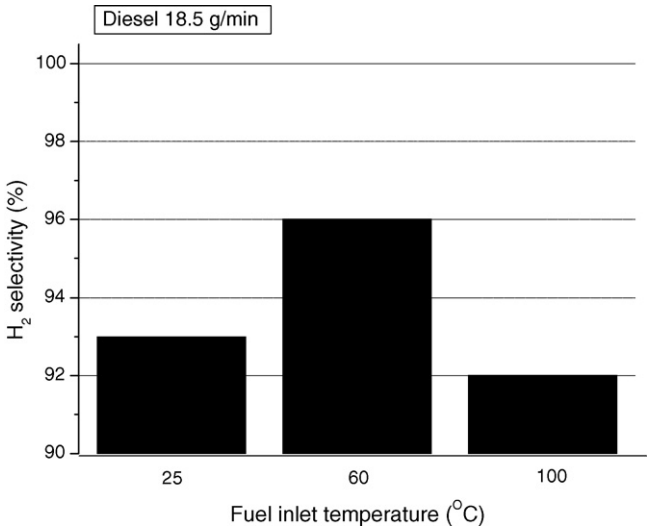

Fig. 11. Effect of the fuel inlet temperature on hydrogen selectivity for autothermal reforming of diesel. Fuel flow = 18.5 g/min, $H_2O/C = 2.5$, $O_2/C = 0.49$, GHSV = 10,800 h^{-1}. The analyzed dry gas samples were collected after ATR2.

Fig. 10 displays the temperatures during operation at a diesel flow of 18.5 g/min at steady-state conditions. A homogeneous ignition of the reactant mixture, aka light off temperature, occurs initially for autothermal reforming of diesel [4]. The ignition increases the temperature in the mixing zone from 300 to 400 °C before reaching equilibrium. These temperature trend results are in good agreement with what has been reported by Kang et al. [9] and by Borup et al. [33]. Kang et al. [9] reports a light off temperature of 250 °C while Borup et al. [33] report a light off temperature of 270 °C for diesel. It can also be noted that steady-state conditions, displayed as stable and flat temperature curves in Fig. 10, were reached approximately 30 min after start-up of the reformer. Also, the repositioning of the air/steam injection holes in the mixing zone seems to have a beneficial effect as no local hot spot or temperature rises were detected in the system.

As steady state was achieved in the reactor system at a fuel flow of 18.5 g diesel/min; the remainder of the operating parameters FIT, H_2O/C and O_2/C were evaluated in order to find the optimal reaction conditions for ATR of diesel. The parameter fuel inlet temperature was evaluated first. Results from Table 3 shows that the FIT has a positive effect on the fuel and oxygen conversion. Also, the FIT promotes the WGS reaction as previously discussed. Therefore, it is interesting to calculate the hydrogen selectivity as a function of FIT to determine at what point the FIT has the highest impact. Fig. 11 shows the influence of varying fuel inlet temperature on the H_2 selectivity (measured after ATR2) at constant fuel flow (18.5 g/min), oxygen-to-carbon ratio ($O_2/C = 0.49$) and steam-to-carbon ratio ($H_2O/C = 2.5$). As seen in the figure, maximum H_2 selectivity (96%) is reached at a fuel inlet temperature of 60 °C. It is unclear why the results point to this trend. No C2- and C4-compounds were noted in the wet reformate after ATR2 at FIT 60 and 100 °C. However, a small amount of coke (coke weight ~0.030 g) was present in the nozzle at fuel inlet temperature 100 °C. Also, it is possible that preheating using high FIT may promote pre-reforming reactions, which can affect the catalyst activity negatively [34]. Nevertheless, the results from Fig. 11 show that the optimum FIT is 60 °C.

As the optimum FIT was determined, the parameter oxygen-to-carbon ratio was next in line to be evaluated. Fig. 12 shows the influence of varying the O_2/C ratio and fuel inlet temperature on the reforming efficiency. As seen in the figure, increasing the fuel inlet temperature has a minor effect on the reforming efficiency, as compared to the O_2/C ratio. A possible explanation to this trend is that the O_2/C ratio has a higher impact on the reforming temperature.

Fig. 13 shows the reforming temperatures measured in the center of the reactor after the foam, ATR1 and ATR2, respectively, varying O_2/C ratios, at constant diesel flow (18.5 g/min), fuel inlet temperature (FIT = 60 °C), and steam-to-carbon ratio ($H_2O/C = 2.5$). As seen in the figure, the oxygen concentration has a high impact and governs the reforming temperature during autothermal reforming. Similar results have been reported by Liu et al. [31]. Furthermore, an O_2/C ratio of 0.52 results in reforming temperatures around 800 °C, which, according to thermodynamic equilibrium calculations, reported in a previous study [8], is unfavorable as it can cause a decrease of predicted hydrogen production and selectivity. Thus, the results from Figs. 12 and 13 show that the optimum O_2/C ratio is 0.49.

As the optimum FIT and O_2/C ratio were determined; the parameter H_2O/C was also evaluated. Fig. 14 shows the influence of varying steam-to-carbon and oxygen-to-carbon ratios on

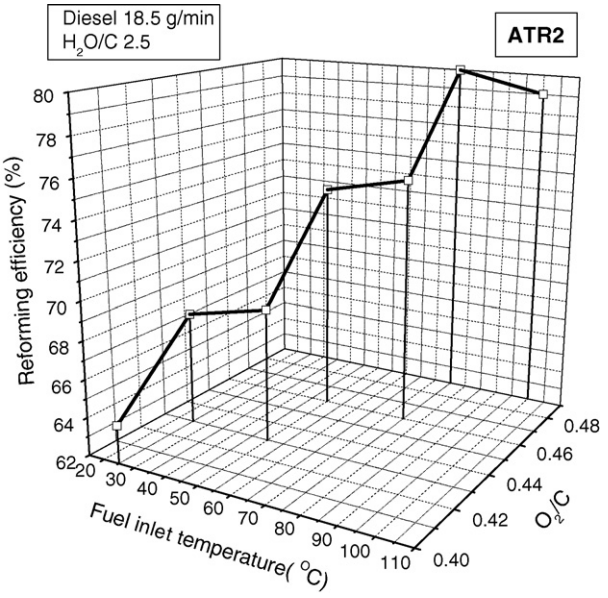

Fig. 12. Comparison of the fuel inlet temperature and O_2/C ratio on the reforming efficiency measured after monolith ATR2 at a constant diesel flow 18.5 g/min and steam-to-carbon ratio $H_2O/C = 2.5$. GHSV = 9900–10,800 h^{-1}.

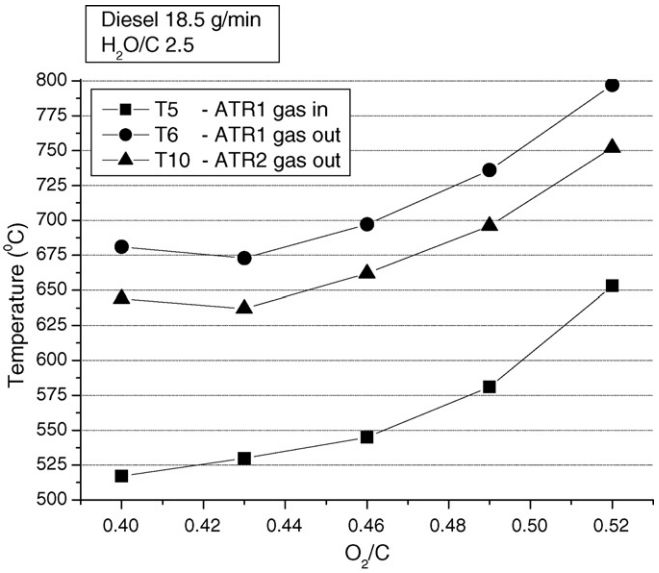

Fig. 13. Temperatures measured after the alumina foam (T5), monoliths ATR1 (T6) and ATR2 (T10) at different O_2/C at constant diesel flow 18.5 g/min, fuel inlet temperature 60 °C and steam-to-carbon ratio H_2O/C = 2.5. GHSV = 9900–10,800 h^{-1} (positions of the thermocouples are shown in Fig. 1).

the H_2 selectivity at constant fuel inlet temperature (FIT = 60 °C). Maximum H_2 selectivity (~96%) is achieved at H_2O/C = 2.5 and O_2/C = 0.49. Further increase of the O_2/C ratio is believed to cause total oxidation of the fuel and as a result the hydrogen selectivity is decreased (Eq. (2)). The H_2O/C ratio has a minor impact on the hydrogen selectivity. In ATR, it is known that the H_2O/C ratio has a minor impact on the reforming temperature compared to the O_2/C ratio. In fact, Liu et al. [31] have shown that a decline in the reforming temperature is noted as the H_2O/C ratio increases. Water is a much weaker oxidant compared to oxygen. Thus, an increase in O_2/C enhances the initial oxidation reactions in ATR, which increases the reforming temperature and furthermore, as seen in Fig. 14, improves the hydrogen selectivity. The results from Fig. 14 show the optimum H_2O/C ratio is 2.5.

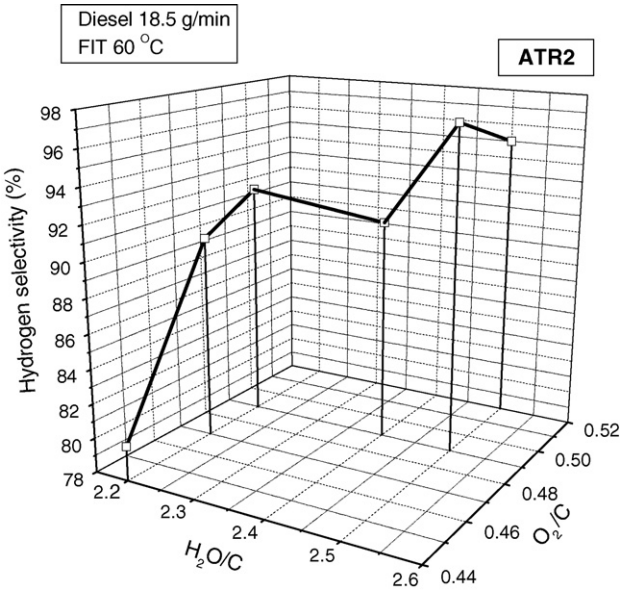

Fig. 14. Comparison of the operating parameters steam-to-carbon ratio (H_2O/C) and oxygen-to-carbon ratio (O_2/C) on the hydrogen selectivity after monolith ATR2, at constant diesel flow 18.5 g/min and fuel inlet temperature (FIT) 60 °C. GHSV = 9900–10,800 h^{-1}.

It was concluded from the experiments running at diesel flow of 18.5 g/min that elevated fuel inlet temperatures (≥60 °C) and a higher degree of fuel dispersion significantly improves the performance of the reformer. Complete fuel conversion, a reforming efficiency of 81% and a H_2 selectivity of 96%, were established at P = 5 kW_e, H_2O/C = 2.5, O_2/C = 0.49 (λ = 0.33) and at a fuel inlet temperature of 60 °C. These operating parameters were found to offer optimal reaction conditions for ATR of diesel.

4.3. Jet A-1 reforming

Fig. 15 shows the temperature profile in the reformer during operation of jet A-1 at 18.5 g/min at steady-state conditions. The temperatures in the mixing zone and after the foam are not different from those obtained operating with diesel fuel. The temperature inside the channels of ATR1 was ~880 °C, which is higher than for the diesel reforming experiments. A high temperature is beneficial during jet fuel reforming because the risk for strong sulfur adsorption on the active sites of the catalyst decreases at temperatures above 800 °C [22]. The oxygen conversion in ATR1 was 97%, regardless of the fuel inlet temperature employed. The temperature inside the channels of ATR2 was 778–806 °C. The oxygen conversion after ATR2 was still 97%, regardless of the fuel inlet temperature employed. For ATR2, the temperature of the effluent was 727–736 °C. As previously discussed, the decrease in temperature can be the result of steam-reforming activity.

The results from jet A-1 reforming again confirm the typical appearance of the autothermal reforming (ATR) temperature profile. Exothermic partial oxidation initiates the ATR, followed by endothermic steam reforming. This temperature trend can be seen in Fig. 15, expressed as the ATR curve. The light off temperature of jet A-1 was approximately 300 °C (not shown in any figure), thus similar to diesel.

Fig. 16 shows results for autothermal reforming of jet A-1 fuel measured after ATR2. It can be seen that an increase of the O_2/C and the fuel inlet temperature improves the fuel conversion and reforming efficiency. A fuel conversion of 76% and a reforming efficiency of 42% are achieved at a fuel inlet temperature of 60 °C (H_2O/C = 2.1, O_2/C = 0.39). A supplementary test was conducted to confirm the initial results and to find the optimal point of the operating parameters. A spontaneous homogeneous autoignition of the reactant mixture ended this experiment after 2 h and 20 min operation. The temperature in the mixing zone first rose slowly from 450 to 500 °C, and then rose instantly from 500 to 1000 °C. Thus, it seems the limiting upper temperature for ignition of jet A-1 is around 500 °C. The autoignition of the fuel can be an indication that too high values of the stochiometric air/fuel ratio (λ) were implemented [4,34]. Prior to the autoignition, the GC analysis showed a steady decrease in the H_2 production (measured after ATR2) from 19 to 12 vol%, regardless of the operating parameters employed. Similar results have been presented by McCoy et al. [27] were SR of kerosene as jet fuel surrogate, were tested over noble metal-based catalyst and a steady decrease of H_2 yield from 30 to less than 10% was noted with time on stream. In this study, carbonaceous substances were detected in the condensate from the reactor effluent. Furthermore, extra long periods of oxygen purging was necessary during shutdown for coke and possibly also sulfur removal, see Eqs. (7)–(9). The observations suggest that catalyst deactivation occurs due to coke deposition and by sulfur poisoning. Coke deposition may have originated from the benzene and toluene, typically present in the fuel [23] and in the reformate [20]. For instance, benzene can form carbon through dehydrogenation [26]. Also, high amounts of C2-compounds (~250 ppm) with an increase over time on stream, were detected in the wet reformate from both monoliths. It is possible that olefins, such as ethylene, are present in the reformate. It has been shown by

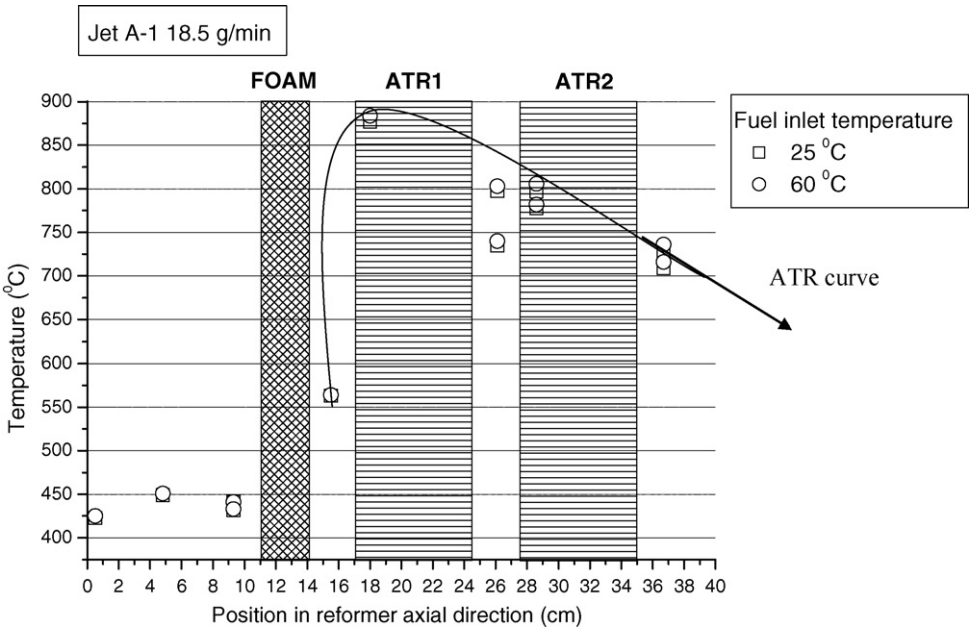

Fig. 15. Temperatures in the reactor during autothermal reforming of commercial jet A-1 at different fuel inlet temperature. Fuel flow = 18.5 g/min, $H_2O/C = 2.1$, $O_2/C = 0.39$, GHSV = 9000 h^{-1} (positions of the thermocouples are shown in Fig. 1). FOAM = zirconia-treated alumina foam, ATR1 = first monolith in line, ATR2 = second monolith in line. The ATR curve shows the thermodynamic trend where the exothermic partial oxidation occurs initially followed by endothermic steam reforming.

Rostrup-Nielsen et al. [35] that olefins, such as ethylene, have higher coking tendency compared to aromatics and paraffin. Olefins can form carbon deposits at temperatures higher than 700 °C [4]. In this study, efforts were made to identify possible C2-compounds formed during jet A-1 reforming. For instance, ethylene, ethane and acetaldehyde were injected into the GC, but could not be separated adequately to enable identification of the samples from the experiments.

Either than coke deposition, the catalyst deactivation can also have occurred by adsorption of S-compounds, such as H_2S and SO_2. As previously discussed, both these sulfur products can be formed in the reformate during autothermal reforming [4]. The presence of H_2S and SO_2 has been reported to cause deactivation of noble metal-based catalyst in autothermal reforming [18–19,22]. In this study, the steady decline of H_2 production; the autoignition of the fuel; the strong exothermic reactions noted; and the extra long period of oxygen purging during shutdown of the reactor; suggest the presence of both coke and sulfur adsorbates.

Ocular inspection of the alumina foam (see Fig. 17) and the front part of ATR1 showed physical deformation and extensive coke deposits. The coke formation may be an indication of pre-reforming reactions where higher hydrocarbons are converted into a mixture of lighter hydrocarbons. Hartmann et al. [34] have shown cases of

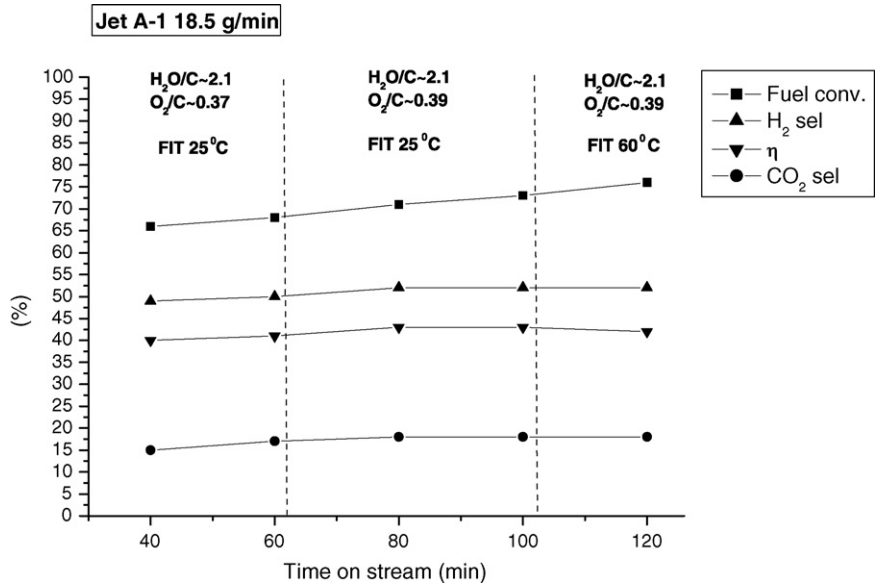

Fig. 16. Jet A-1 autothermal reforming. Results show fuel conversion, reforming efficiency, and H_2 and CO_2 selectivities vs. time on stream at different O_2/C and fuel inlet temperatures. Fuel flow = 18.5 g/min and $H_2O/C = 2.1$. The analyzed gas samples were taken after ATR2.

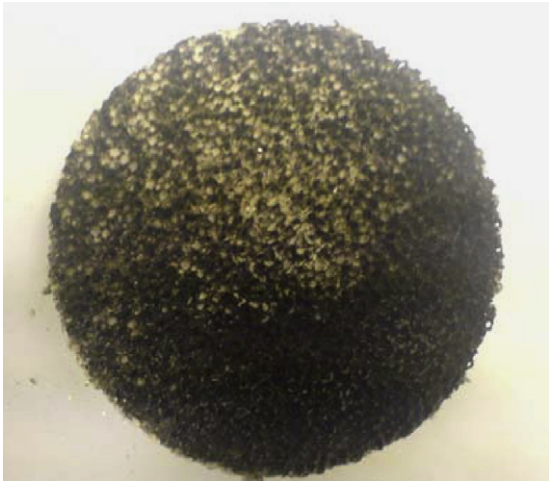

Fig. 17. Zirconia-treated alumina foam from autothermal reforming of jet A-1, 18.5 g/min, after final experiment.

pre-reforming where if the reactant mixture is not homogeneously blended; if wrong operating parameters are employed; the tendency of coke formation is high. In this study, no local hot spots were detected in the mixing zone that indicated poor reactant mixing. Furthermore, the coke noted suggests that a higher H_2O ratio than 2.1 should be employed in order to suppress the carbon formation.

Coke deposits were also spotted inside the nozzle filter system and swirl channel. The measured coke weight was ~0.400 g. Similar damage on the reactor system has been reported by Pasel et al. [20].

A summary of the results from jet A-1 reforming is to be found in Fig. 18. Despite the comparatively high aromatic and sulfur content in the jet fuel, a fuel conversion of 76%, a reforming efficiency of 42%, and an H_2 selectivity of 52% were achieved after ATR2. The low CO_2 selectivity 18% is due to low amount of CO_2 present in the analyzed dry reformate sample (~4 vol% not shown in any figure), which indicates incomplete combustion of the jet fuel. A CH_4 concentration of 4.8 vol% is obtained, which is quite high for jet A-1 reforming in comparison what has been reported earlier in the open literature for ATR of sulfur free jet fuel surrogates [20]. However, McCoy et al. [27] reports for SR of sulfur and aromatic doped kerosene as jet fuel surrogate that a high level of methane was obtained. The total amount of methane was not specified. They suggest a synergistic effect between the sulfur and aromatics in the fuel may have promoted the high production of CH_4. Similar observations were made by Kaila et al. [22]. They report that the presence of H_2S during reforming of surrogate diesel could have promoted the decomposition of aromatics, e.g. toluene by cleavage of methyl groups leading to higher production of CH_4 [16]. The high methane formation noted for ATR of jet A-1 in this study, should also be an indication that too low H_2O and O_2/C ratios were implemented. In general, methane formation decreases with higher H_2O and O_2/C ratios [4]. Nevertheless, the poisoning effect of CH_4 for PEFC is very small as the fuel cell can tolerate up to 5 vol% methane without any detrimental effect on the performance [4].

The oxygen conversion is not affected in the presence of sulfur. Similar results have been reported by Kaila et al. [16]. Finally, despite a reforming temperature of above 800 °C inside the channels of ATR1 the catalyst appeared to have been deactivated by sulfur.

It was concluded from the experiments on jet A-1 reforming that the high aromatic and sulfur load in the fuel should have had a detrimental effect on the reformer performance and durability. A steady decline of the hydrogen production was noted with time on stream. Furthermore, an autoignition of the fuel occurred. Coke deposits were also spotted on the nozzle, alumina foam and catalyst. All these results suggest that it is highly recommended to employ a pretreatment of the jet fuel, e.g. desulfurization step, prior to the reformer. Also, a higher H_2O ratio than 2.1 should be employed in order to reduce the coke and methane formation.

4.4. Overall results: REF1 and REF2

Fig. 18 shows the overall results for REF1 (the 1st generation reformer) running on diesel in comparison to REF2 (the 2nd generation reformer) running on diesel and jet fuel. The results show that REF2 for diesel reforming at 18.5 g fuel/min exhibited the best performance in terms of fuel conversion, reforming efficiency and H_2 selectivity. The graph also shows that the in-house prepared 1 wt% Rh monolithic catalyst tested in REF1 resulted in 2 vol% higher H_2 production in comparison with the commercial noble metal catalyst tested in REF2. Catalyst development for REF2 will be discussed in a future paper.

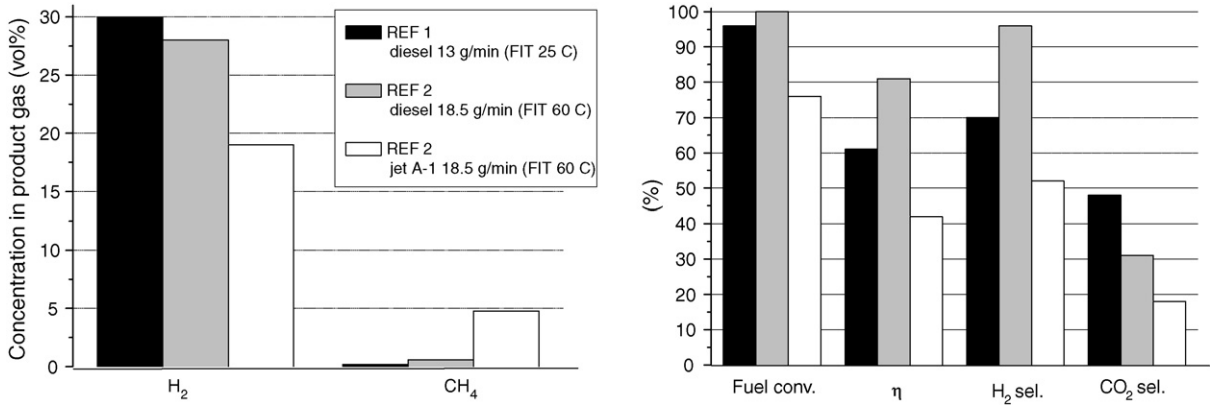

Fig. 18. Overall results for the 1st generation reformer (REF1) in comparison to the 2nd generation reformer (REF2). FIT = fuel inlet temperature. Operational conditions for REF1 diesel: fuel flow = 13 g/min, FIT = 25 °C, P = 3 kW_e, H_2O/C = 2.0, O_2/C = 0.40, GHSV = 8700 h^{-1} [6]. Operational conditions for REF2 diesel: fuel flow = 18.5 g/min, FIT = 60 °C, P = 5 kW_e, H_2O/C = 2.5, O_2/C = 0.49, GHSV = 10,800 h^{-1}. Operational conditions for REF2 jet A-1: fuel flow = 18.5 g/min, FIT = 60 °C, P = 5 kW_e, H_2O/C = 2.1, O_2/C = 0.39, GHSV = 9000 h^{-1}.

5. Summary and conclusions

The objective of this study was to characterize and optimize an autothermal reformer for operation with commercial diesel fuel or jet fuel. The parameters investigated were variation of the fuel inlet temperature, fuel flow and H_2O/C and O_2/C ratios. Two commercial noble metal-based catalysts supported on monolithic cordierite (900 cpsi) were tested. Steady-state conditions and reproducible results were obtained throughout the experiments. Results from this study show that:

- The 2nd generation reformer had a significantly higher operating efficiency and system stability during diesel autothermal reforming compared to the 1st generation reformer.
- It is difficult to find single-fluid pressurized-swirl nozzles for diesel reforming that can guarantee good spray quality over the entire flow range. At low fuel flows, bigger fuel droplets are generated, which has a negative impact on the reactant mixing and the catalyst performance. This problem needs to be addressed and solved in order for mobile fuel cell applications to reach commercialization.
- Complete fuel conversion was achieved using two noble metal-based monolithic catalysts for all diesel fuel loads tested.
- Elevated fuel inlet temperature improved the performance of the reformer significantly in terms of fuel and oxygen conversions at low diesel fuel loads, 13 g/min (3 kW_e), particularly after the first reforming catalyst.
- Optimal operating parameters for autothermal reforming of commercial diesel at a fuel flow of 18.5 g/min (5 kW_e) were determined. They are as follows: fuel inlet temperature FIT = 60 °C, steam-to-carbon ratio $H_2O/C = 2.5$ and oxygen-to-carbon ratio $O_2/C = 0.49$.
- High aromatic and sulfur concentrations present in the jet fuel had a detrimental effect on the reformer's performance and durability.

In conclusion, our results indicate possibilities for the developed catalytic reformer to be used in onboard fuel cell applications for energy-efficient hydrogen production from diesel fuel.

Acknowledgements

The Foundation for Strategic Environmental Research (MISTRA) and the Swedish Energy Agency (Energimyndigheten) are gratefully acknowledged for financial support.

Nomenclature

ATR	autothermal reforming
ATR1	commercial monolithic noble metal catalyst, first in line
ATR2	commercial monolithic noble metal catalyst, second in line
CFD	computational fluid dynamics
F	molar flow (mol/min)
FIT	fuel inlet temperature (°C)
FID	flame ionization detector
GC	gas chromatography
GHSV	gas hourly space velocity (h^{-1})
H_2O/C	steam-to-carbon ratio
LHV	lower heating value (MJ/kg)
O_2/C	oxygen-to-carbon ratio
P	electric power output for a polymer electrolyte fuel cell (kW_e)
PEFC	polymer electrolyte fuel cell
PO	partial oxidation
REF1	1st generation catalytic autothermal reformer
REF2	2nd generation catalytic autothermal reformer
SR	steam reforming
T#	thermocouple number
TCD	thermal conductivity detector
WGS	water-gas shift reaction
η	reformer efficiency (%)

References

[1] J.D. Holladay, J. Hu, D.L. King, Y. Wang, Catal. Today 139 (2009) 244–260.
[2] S. Specchia, A. Cutillo, G. Saracco, V. Specchia, Ind. Eng. Chem. Res. 45 (2006) 5298–5307.
[3] T. Aicher, L. Griesser, J. Power Sources 165 (2007) 210–216.
[4] G. Kolb, Fuel Processing, Wiley-VCH Verlag GmbH & Co., KGaA, Weinheim, 2008.
[5] Z. Porš, J. Pasel, A. Tschauder, R. Dahl, R. Peters, D. Stolten, Fuel Cells 8 (2) (2008) 129–137.
[6] G. Kolb, T. Baier, J. Schürer, D. Tiemann, A. Ziogas, H. Ehwald, P. Alphonse, Chem. Eng. J. 137 (2008) 653–663.
[7] M. Nilsson, X. Karatzas, B. Lindström, L.J. Pettersson, Chem. Eng. J. 142 (2008) 309–317.
[8] M. Nilsson, Hydrogen generation for fuel cells in auxiliary power systems, PhD thesis, KTH, Department of Chemical Engineering and Technology, TRITA-CHE Report 2009:7, ISBN 978-91-7415-245-6 (2009).
[9] I. Kang, J. Bae, S. Yoon, Y. Yoo, J. Power Sources 172 (2007) 845–852.
[10] R.B. Bird, W.E. Stewart, E.N. Lightfoot, Transport Phenomena, 2nd ed., John Wiley & Sons Inc., New York, 2002.
[11] The Swedish Petroleum Institute, SPI, www.spi.se, last visited 2009-01-22, last updated 2008-12-01.
[12] Dieselnet, http://www.dieselnet.com, last visited 2009-01-22.
[13] T. Edwards, L.Q. Maurice, J. Prop. Power 17 (2) (2001) 461–466.
[14] W.G. Dukek, J.I. in, M. Kroschwitz, Howe-Grant (Eds.), Kirk-Othmer Encyclopedia of Chemical Technology, 4th ed., Wiley-Interscience Publication, New York, 1992.
[15] Air BP, Handbook of Products, www.bp.com, last visited 2009-01-22.
[16] J. Latz, R. Peters, J. Pasel, L. Datsevich, A. Jess, Chem. Eng. Sci. 64 (2008) 288–293.
[17] D.D. Link, P. Zandhuis, Fuel 85 (2006) 451–455.
[18] S. Cimino, R. Torbati, L. Lisi, G. Russo, Appl. Catal. A 360 (2009) 43–49.
[19] P.K. Cheekatamarla, A.M. Lane, J. Power Sources 152 (2005) 256–263.
[20] J. Pasel, J. Meißner, Z. Porš, R.C. Samsun, A. Tschauder, R. Peters, Int. J. Hydrogen Energy 32 (2007) 4847–4858.
[21] X. Cheng, Z. Shi, N. Glass, L. Zhang, J. Zhang, D. Song, Z.S. Liu, H. Wang, J. Shen, J. Power Sources 165 (2007) 739–756.
[22] R.K. Kaila, A. Gutiérrez, A.O. Krause, Appl. Catal. B 84 (2008) 324–331.
[23] Environmental Science & Technology Centre, Database, Oil Properties Jet A-1, http://www.etc-cte.ec.gc.ca/etchome_e.html, last visited 2009-10-01.
[24] I. Tesseraux, Toxicol. Lett. 149 (2004) 295–300.
[25] C. Palm, P. Cremer, R. Peters, D. Stolten, J. Power Sources 106 (2002) 231–237.
[26] M. Flytzani-Stephanopoulos, G.E. Voecks, Int. J. Hydrogen Energy 8 (1983) 539–548.
[27] A.C. McCoy, M.J. Duran, A.M. Azad, S. Chattopadhyay, M.A. Abraham, Energy Fuels 21 (2007) 3513–3519.
[28] L. Shi, D.J. Bayless, Int. J. Hydrogen Energy 33 (2008) 1067–1075.
[29] B. Lenz, T. Aicher, J. Power Sources 149 (2005) 44–52.
[30] S. Yoon, I. Kang, J. Bae, Int. J. Hydrogen Energy 33 (2008) 4780–4788.
[31] D. Liu, T.D. Kaun, H. Liao, S. Ahmed, Int. J. Hydrogen Energy 29 (2004) 1035–1046.
[32] A. Abu-Jrai, A. Tsolakis, K. Theinnoi, A. Megaritis, S.E. Golunski, Chem. Eng. J. 141 (2008) 290–297.
[33] R.L. Borup, M.A. Inbody, T.A. Semelsberger, J.I. Tafoya, D.R. Guidry, Catal. Today 99 (2005) 263–270.
[34] L. Hartmann, K. Lucka, H. Köhne, J. Power Sources 118 (2003) 286–297.
[35] J.R. Rostrup-Nielsen, T.S. Christensen, I. Dybkjaer, Stud. Surf. Sci. Catal. 113 (1998) 81–95.